Int J Adv Manuf Technol (2007) 34:1111–1119
DOI 10.1007/s00170-006-0678-0

ORIGINAL ARTICLE

Modeling and simulation of wire feed rate for steady current and pulsed current gas metal arc welding using 317L flux cored wire

P. K. Palani · N. Murugan

Received: 16 October 2005 / Accepted: 11 May 2006 / Published online: 18 August 2006

Abstract Wire feed rate plays a vital role in determining the weld characteristics in gas metal arc welding (GMAW). The wire feed rate is affected by any change in welding current in the case of steady current GMA welding and by any change in frequency, peak current, base current and duration of peak and base currents in the case of pulsed GMA welding. To predict the wire feed rate for any set of these parameters, a mathematical model was developed from the results obtained by conducting experiments. Electrode resistance heating constant and arc resistance heating constant were also determined by fitting a regression model. The above parametric constants have been used to simulate the wire feed rates for pulsed GMA welding for different pulse parameters using MATLAB. The effects of pulse parameters on the burnoff factor and burnoff rates were also analysed. The investigation was carried out using AWS 5.22–95 filler wire of size 1.2 mm diameter and the base metal used was IS:2062 structural steel plate of 20 mm thickness. An argon and 5% CO_2 gas mixture at a flow rate of 16 l/min was used for shielding throughout the welding.

Keywords Welding current · Wire feed rate · Regression analysis · Pulse parameters · Arc resistance heating constant · Wire resistance heating constant

P. K. Palani (✉)
Faculty of Mechanical Engineering,
Government College of Technology,
Coimbatore 641 013, India
e-mail: pkpalaniku@yahoo.com

N. Murugan
Coimbatore Institute of Technology,
Coimbatore 641 014, India
e-mail: drmurugan@yahoo.com

1 Introduction

GMAW is an arc welding process, which incorporates the automatic feeding of a continuous, consumable electrode that is shielded by an externally supplied gas. GMA welding can be used for most types of metals: steel, stainless steel, as well as aluminum. Despite its wide applications and advantages [1–10], the GMAW process has some limitations regarding the control of metal transfer [11]. For instance the industrial relevance of steady current welding is limited because of positional limitations with steel [2, 12–14]. These limitations have been partially overcome with the advent of pulsed technologies. However, the introduction of pulsed GMAW exposed the need for new parameter settings in addition to those already existing in conventional GMAW [15, 16]. Hence it is not so easy to select the values of those new parameters since for each welding condition (base material, electrode material, electrode diameter, shielding gas type, etc.) there is an optimum parameter combination; this has been one of the main reasons for lack of popularity of pulsed GMA welding in industries. In many instances, parameter selections are based on trial and error or on reference to a manual. However, with increase of mechanization and automation, the selection of welding procedures must be more specific to ensure that adequate weld bead quality is obtained [17]. Thus simple procedures for calculation and selection of welding parameters are demanded so that the industries can be fully benefited by this versatile process. Though there exists power sources with synergic commands built into their circuits, the system has a limitation since it employs a linear relationship between wire feed rate and mean current [11, 18, 19]. Among the GMAW process parameters, wire feed rate plays a major role in determining the values of the other parameters. Therefore, when the wire feed rate is

modeled properly, selection of the remaining process parameters can be done without much difficulty. Therefore, the main objectives of this work are to (i) model the wire feed rate of steady current GMA welding by conducting experiments, (ii) determine the arc heating melting constant (α) and wire resistance heating constant (β), and (iii) simulate the effect of different pulse parameters on wire feed rate for pulsed GMAW using these constants (α and β), which would enable the welders and researchers to understand the process in a better way.

2 Wire feed rate

For successful operation, the GMAW process has two basic requirements, namely, (1) the wire feed speed [W] must be balanced with the burn-off rate to maintain a constant arc length, and (2) there must be a stable transfer of metal from the electrode wire to the weld pool [5]. Good arc stability is achieved under good metal transfer conditions, particularly when the wire feed rate is exactly matched by the wire-melting rate [4, 5, 20]. Low wire feed rate causes melt back, and a high feed rate can cause the arc to extinguish through short-circuiting [21]. Wire feed rate and travel speed are shown to be only controlling factors for obtaining good penetration [22]. Also, in GMAW, the current depends on the rate at which the wire is fed into the arc [5, 9, 23–25].

Most of the wire feed rate models are based on experiments and only a few on computations of arc and resistance heating of the wire during welding. When all other variables are constant, wire feed speed will become a function of current and the wire feed rate may be predicted using an equation of type $W_f=S_{ml}+k$, where W_f=wire feed rate in m/min, S_m=slope and k=intercept [5, 26].

2.1 Wire feed rate for steady current GMA welding

To fulfill the above-mentioned two basic requirements, an expression for the wire feed rate must be found. The authors have adopted two approaches to model the wire feed rate. One is to conduct experiments to fit the equation relating welding current and wire feed rate, and the other is to use the results of this experiments to determine the constants of proportionality for anode or cathode heating and of electrical resistance heating.

2.2 Plan of investigation

The investigation was carried out adapting the following steps:

1. Identifying the important process parameters
2. Finding the limits of the process parameters
3. Conducting experiments
4. Recording the response
5. Development of mathematical model
6. Estimation of the coefficients of the model
7. Checking the adequacy of the model developed
8. Analysis of results

2.3 Identifying the important process parameters

Trial runs were carried out by varying one of the process parameters and keeping the rest of them at constant values. The working range of each process variable was decided upon by inspecting the bead for smooth appearance and the absence of any visible defects, viz., surface porosity, undercut, etc.

2.4 Finding the limits of the process parameters

On the basis of preliminary experiments conducted for proper bead configurations, the range of welding current, nozzle-to-plate distance and welding speed were found to be between 170 A to 300 A, 15 mm to 25 mm, and 25 cm/min to 50 cm/min, respectively. The gas flow rate was maintained at 16 l/min.

The values of welding parameters, their units and their notations are given in Table 1.

2.5 Experimentation

Experiments were conducted by using a mechanized welding system as per the conditions set in Table 1. The experimental set up used to carry out the experiments is shown in Fig. 1. Wire feed rate observations were made by making bead on plate welds of 150 mm length. The power source used was a Unimacro Esseti 501C Synergic MIG welder. A constant arc length was achieved by matching the wire feed speed with burn off rate by suitably adjusting the wire feed rates by trial and error. The investigation was carried out for AWS 5.22-95 (flux cored) filler wire of diameter 1.2 mm and the base metal used was IS:2062 structural steel plate of 20 mm thickness, with shielding gas containing 95% argon and 5% CO_2.

Table 1 Welding parameters and their units

Parameter	Unit	Notation	Value
Welding current	A	I	170–250
Nozzle-to-plate distance	mm	N	20.0
Welding speed	cm/min	S	25.0
Electrode extension	mm	L	20.0

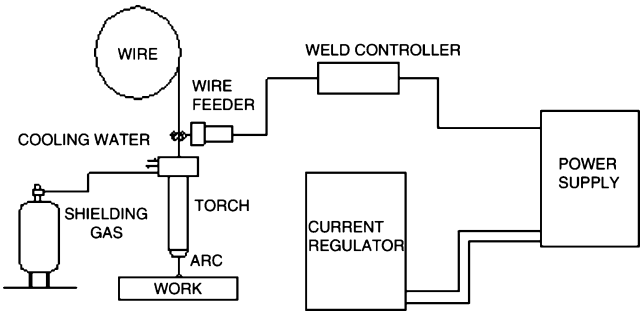

Fig. 1 Experimental setup for GMAW process

2.6 Recording the response

Several trial experiments were conducted to locate the approximate region of wire feed rate for stable arc for a given current. From the trials, five current values were selected and weld runs were made. The recorded values of wire feed rate (W_f) are given in Table 2.

2.7 Development of regression model

The response function representing wire feed rate can be expresses as [27–29]:

$$W_f = S_m I + k \tag{1}$$

where W_f=wire feed rate in m/min, I=welding current (A), S_m=slope and k=intercept.

Based on the experimental results (Table 2), the regression equation was found to be,

$$W_f = -6.92 + 0.0860 * I \tag{2}$$

Similar equations have also been obtained by others [4, 5, 20, 24, 30–33].

2.8 Checking the adequacy of the model

The estimated coefficients obtained above were used to construct the model for the response parameter. One criterion that is commonly used to illustrate the adequacy of a fitted regression model is the coefficient of determination (R^2), which is given by Eq. 3 [34]:

$$R^2 = \frac{SSR}{SST} = \frac{\sum \left(\widehat{Y} - \overline{Y}\right)^2}{\sum \left(Y_i - \overline{Y}\right)^2} = 1 - \frac{SSE}{SST} \tag{3}$$

SSR Regression sum of squares
SST Total sum of squares
SSE Error sum of squares
$\widehat{Y}$ Estimated value of the response using the regression model
Y_i Observed value of the response
$\overline{Y}$ Mean of observed values of the response

For the model developed, the calculated R^2 value was 29.584/29.592=99.9%, which indicates that the regression model is quite adequate and that 99.9% of the variation in the response has been explained by this regression model.

Table 2 Recorded values of wire feed rates

Trial no.	Current I (A)	Wire feed rates, m/min		Average wire feed rate (m/min)
		W_1	W_2	
1	170	7.8	7.6	7.7
2	190	9.3	9.5	9.4
3	210	11.2	11.2	11.2
4	230	13.0	12.6	12.8
5	250	14.5	14.7	14.6

3 Determination of α and β

3.1 Theoretical background

To investigate the basic requirements for optimum metal transfer mentioned in the previous section, an expression for the burn-off rate must be found. This burn-off rate is determined by the amount of heat (J/sec) being transmitted to the wire divided by the energy (J/m) needed to melt the wire [22, 35–37]. The heat transmitted to the wire is composed of the following elements:

(i) Wire resistance heating: $L\sigma I^2/A$, where L=electrode extension, mm; σ=wire resistivity, Ωm; I=current, A; and A=wire cross-sectional area, mm^2.
(ii) Anode voltage drop which imparts kinetic energy to the electrons, $V_a I$, where V_a=anode voltage drop, V.
(iii) Temperature of electrons as they enter the anode. This is proportional to the arc current and therefore can be represented as a voltage drop:

$$\frac{3}{2} k \frac{T_e}{e} = V_T I \tag{4}$$

where k=Boltzman constant, eV/K; T_e=temperature of electrons, K; e=electron charge, C; and V_T=electron thermal voltage, V.
(iv) Anode work function φ_a, eV. The potential energy converted by electrons as they enter the anode: $\varphi_a I$.

The total energy needed to melt and detach a unit volume of wire (H_{melt}) can also be expressed as the energy required to raise its temperature from ambient to the melting point, melt it (heat of fusion), raise the part of it to its boiling point and

vaporize a small amount. Hence, for smooth weld bead deposition, the following energy balance must be satisfied:

$$AWH_{\text{melt}} = (\varphi_a + V_a + V_T)I + L\sigma I^2/A \tag{5}$$

$$W = \frac{(\varphi_a + V_a + V_T)I}{AH_{\text{melt}}} + \frac{L\sigma I^2}{A^2 H_{\text{melt}}} \tag{6}$$

where W is the wire feed rate in mm/sec.

Since resistivity is not very sensitive to current [12], Eq. 6 can be written as:

$$W = \alpha I + \beta L I^2 \tag{7}$$

where W=wire feed rate, mm/sec; L=electrode extension, mm; α=factor accounting for localized arc heating at the wire tip; and β=factor describing resistance heating along wire length [21, 22].

This general equation has also been verified experimentally by Halmoy and Amson [22]. The above equation was also used by other researchers [2, 21] in their studies. The values of the above parametric constants (α and β) vary from material to material and their size, composition, etc. For instance, the experimental values of α and β for 1.2 mm dia carbon steel wires are 0.3 mm/Asec and 5×10^{-5} $A^{-2}sec^{-1}$, respectively. For aluminum, α is 0.75 mm/Asec and β is negligible [2], and for mild steel wire (1.0 mm dia) the values are $\alpha\approx0.47$ mm/Asec and $\beta\approx10.02\times10^{-5}$ $A^{-2}sec^{-1}$ [38]. Louriel and Scotti [11] found for AWS ER 4043 wire shielded under pure Ar the values of $\alpha=12.8\times10^{-4} m.s^{-1}A^{-1}$ and $\beta=-8.84\times10^{-5}$ $A^{-2}.s^{-1}$.

In this study, the authors used the results of the experiment to calculate electrode extension heating factor (I*L, mm.A) and burn-off rate (feed rate/current, mm/A.s).

3.2 Regression model for electrode burn-off rate

Based on the above results, electrode extension heating factor (I*L) and burn-off rate (wire feed rate/current) were calculated. A regression analysis was performed and the above data is fit as shown in Fig. 2. The regression equation is found to be:

$$\text{wire feed rate}(\text{mm}/\text{sec})/\text{current} = 0.2998 + 0.000138\ I * L \tag{8a}$$

$$\text{wire feed rate}(\text{m}/\text{min}) = 0.017988 * I + 8.28 \times 10^{-6} * I^2 * L \tag{8b}$$

3.3 Checking the adequacy of the model developed for burn-off rate

For the model developed the calculated R^2 value was 98.9% with *R-Sq*(adj)=98.5% which indicates that the regression model is quite adequate and that 98.9% of the variation in the response has been explained by this regression model. The validity of the equation developed was further tested by drawing scatter diagrams as shown in Fig. 3. The diagram of Fig. 3 indicates that the predicted and the observed values of the wire feed rate are scattered close to a 45° line, passing through the origin, indicating an almost perfect fit of the developed empirical model.

Hence, the values of α and β are 0.2998 mm/A/sec and 0.000138 A^{-2} sec^{-1}, respectively.

3.4 Conducting conformity tests to verify the values of heating factors (α and β)

The calculated α and β values were also verified experimentally. Four weld runs were made at different current levels with two different electrode extensions. The results of the confirmation experiments are given in Table 3. The wire feed rates predicted using the above factors gave satisfactory arc stability and weld bead appearance.

4 Wire feed rate for pulsed current GMA welding: state of the art

For pulsed GMA welding, Eq. 7 can not be used directly since the current is not constant. Therefore, for a square wave current, the wire feed rate (W) is given by [21, 22]:

$$W = \int_0^T W(t)dt = (W_p T_p + W_b T_b)F \tag{9}$$

where,

F=pulse frequency (Hz);

$$W_p = \alpha I_p + L\beta I_p^2 \tag{10}$$

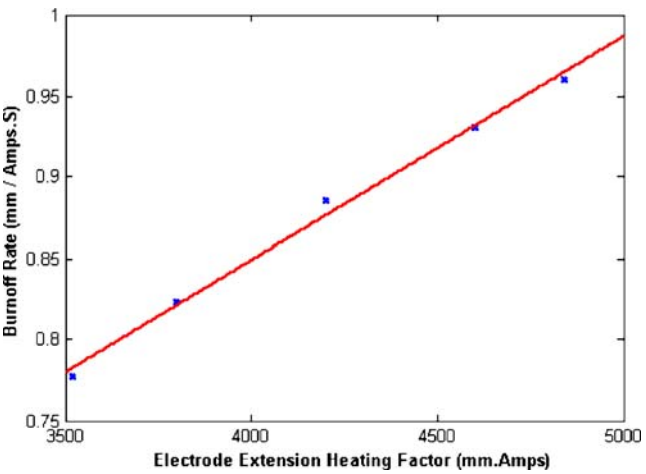

Fig. 2 Burn-off rate vs electrode extension heating factor (the intercept equals α and the line slope equals β)

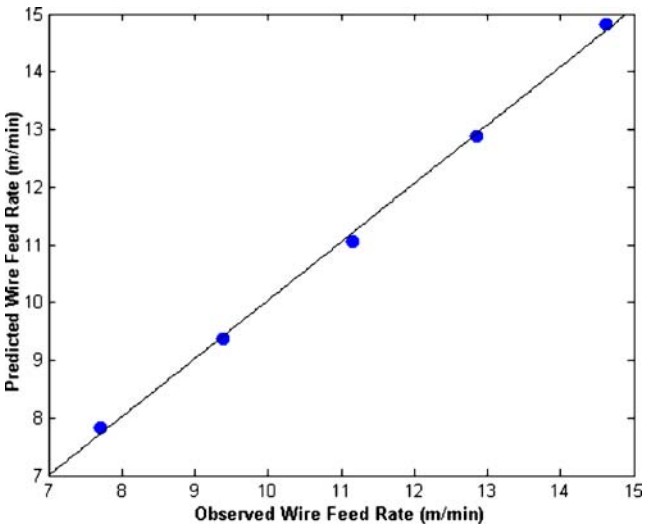

Fig. 3 Scatter plot for experimental feed rate and predicted feed rate based on the calculated α and β

(from Eq. 7);

$$W_b = \alpha I_b + L\beta I_p^2 \tag{11}$$

(also from Eq. 7); T_b=base current duration (s); and T_p=peak current duration (s).

Substituting Eqs. 10 and 11 in Eq. 9, the following equation is obtained [22, 31, 39]:

$$W = \alpha I_{av} + \beta LF\left(I_p^2 T_p + I_p^2 T_b\right) \tag{12}$$

At low mean currents, resistance heating due to background current is negligible. For example, when I_{av} is 100 A, it is only 5% of the total resistance heating [39], consequently, the relation can be simplified to Eq. 13:

$$W = \alpha I_{av} + \beta LF I_p^2 T_p \tag{13}$$

Similarly, Allum and Quintino [40] used Eq. 14 to predict the burn-off rates for Bostrand LW1 wires neglecting ohmic heating during the background period, i.e.

$$W = \alpha I_{av} + \beta L\delta F \tag{14}$$

where δ is the detachment parameter $I_p^2 T_p$, and the authors have used α=0.27 mmA^{-1}sec^{-1}, β=5.93×10^{-5} A^{-2} sec^{-1}, L=15 mm, δ=490 A^2 sec and I_{av}/F=2 A/Hz for their calculations.

However, it can be noted that Amin [5] discarded the joule heating term and used $W=\alpha I_{av}$ as the basis for the 'synergic' MIG process, which is often incorporated in synergic MIG welding equipment. But this approach works over a limited current range and an expression to include joule heating effect is required if the current range is to be extended [22].

Allum [2] adopted a different approach to determine the wire feed speed, which is given by Eq. 15:

$$W(\text{pulse}) = W(DC\ \text{equiv}) + \beta Lx(1-x)I_e^2 \tag{15}$$

where,

$$W(DC\ \text{equiv}) = \alpha I_{av} + \beta I_{av}^2 \tag{16}$$

x=fractional duration of peak ($T_p.F$) and $I_e=I_p-I_b$=excess current.

From Eq. 15 it is apparent that the burn off rate in pulse welding is higher than DC steady current welding for the same equivalent current. However, Rajasekaran [20] has reported that the burn-off characteristic line of steady current GMAW intersects with the burn off characteristic line of pulsed GMAW at the transition current and also that the burn off rate per ampere is more than the steady current GMAW when the average currents are above the spray current level (i.e. burn off rate per ampere is less than the steady current GMAW for the average currents below the spray current level).

Table 3 Results of Confirmation Experiments

Expt. no.	Current (Amps)	Extension (mm)	Actual feed rate** (m/min)	Predicted wire feed rate (m/min)		Error in prediction		Remarks
				Model 1 (Eq. 2)	Model 2 (Eq. 8b)	Model 1	Model 2	
1	170	20	7.70	7.70	7.84	0.00	0.14	Stable arc and good bead appearance
2	176	20	8.21	8.22	8.30	0.01	0.09	Stable arc and good bead appearance
3	190	20	9.40	9.42	9.40	0.02	−0.00	Stable arc and good bead appearance
4	210	20	11.20	11.14	11.08	−0.06	−0.11	Stable arc and good bead appearance
5	230	20	12.80	12.86	12.89	0.06	0.09	Stable arc and good bead appearance
6	244	20	14.15	14.06	14.25	−0.09	0.10	Stable arc and good bead appearance

**As appear in the display of MIG welding equipment

5 Simulation of wire feed rate for pulsed current GMA welding

The wire feed rate for pulsed GMA welding is predicted using Eq. 15 and simulated and presented in Figs. 4, 5, 6, 7, 8, 9, 10, 11, 12.

As previously mentioned, wire feed rate for the pulsed GMA process is affected by the pulse structure, viz., peak current (I_p), peak duration (T_p), base current (I_b), base duration (T_b) and frequency (F) [4, 41, 42]. Influence of these pulse parameters on burn-off rate for a given average current is simulated by varying I_p, T_p and T_b keeping the base current at 80 A.

Figure 4 shows the influence of pulse parameters on wire feed rate (burnoff rate). It can be observed that the burn-off rate in pulsed GMAW is higher than that in steady current welding for the same equivalent current (intercept SC on the burn-off rate axis indicates the burn-off rate for steady current welding).

It is also evident that the burn-off rate increases with increase in burn-off factor (γ), which is defined [2] as:

$$\gamma = x(x-1)I_e^2 = \frac{W(\text{pulse}) - W(\text{steady})}{\beta L} \qquad (17)$$

Figures 5, 6, 7 depict the influence of fractional duration of peak (x=T_p.F) and excess current (I_e=I_p−I_b) on the burn-off factor (γ) for various values of peak current.

It can be observed from these figures that the maximum burn-off rate is achieved when x=0.5 and when excess current is largest. It is interesting to note that, for a given peak time, when the frequency is increased, the burn-off rate increases to a maximum value but further increase in frequency reduces the burn-off rate.

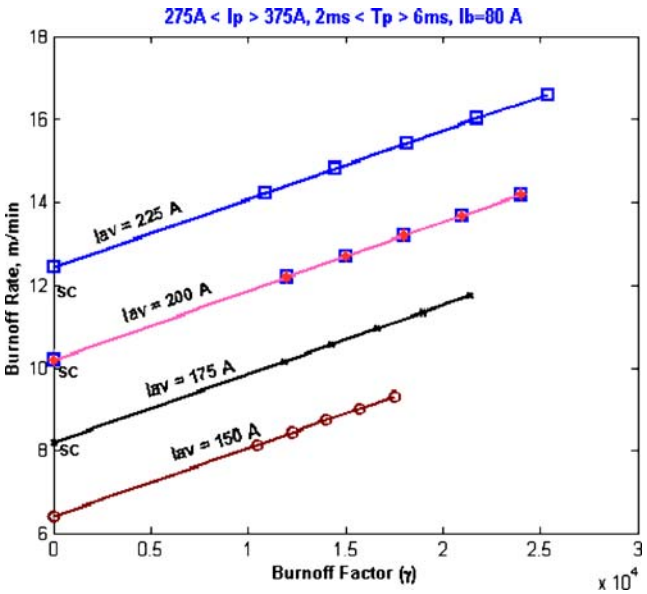

Fig. 4 Influence of pulse parameters on burn-off rate using electrode extension of 20 mm, contact to work distance of 20 mm for 317 L wire, and size 1.2 mm under Ar/5% CO_2. SC indicates the burn-off rate at steady current (simulated results)

5.1 Effect of peak pulse parameters on wire feed rate

Figure 8 shows the relationship between average current and wire feed rate for various peak parameters. It can be observed that for a given average current, the feed rate is influenced by peak parameters. The wire feed rate increases as the peak current and duration increases. However, it is interesting to note that at higher average currents, the wire feed rates are higher for low peak parameters than the high peak parameter values. For example, at I_{av}=340 A, for I_p=250 A and T_p=4 msec, wire feed rate=30.4 m/min, for I_p=300 A and T_p=4 msec, wire feed rate = 27.5 m/min, and for I_p=350 A and T_p=4 msec, wire feed rate = 26.5 m/min.

5.2 Effect of frequency on wire feed rate

Figures 9, 10, 11 depict the influence of frequency on wire feed rate. The simulation results indicate that the wire feed rate increases as the frequency is increased. Also, it can be inferred that the higher the peak values are, the higher the wire feed rates are. However, when the peak duration is increased, the feed rate increases to a maximum value and then starts to decrease and this may be due to the fact that the base current changes its sign at one point, which is not a desirable condition.

5.3 Effect of base current on wire feed rate in pulsed GMAW

Base current is the lower of the two currents of pulse waveform. It is selected in such a way that it is sufficient to maintain the arc. Several authors had neglected the effect of base current in analysing the metal transfer characteristics

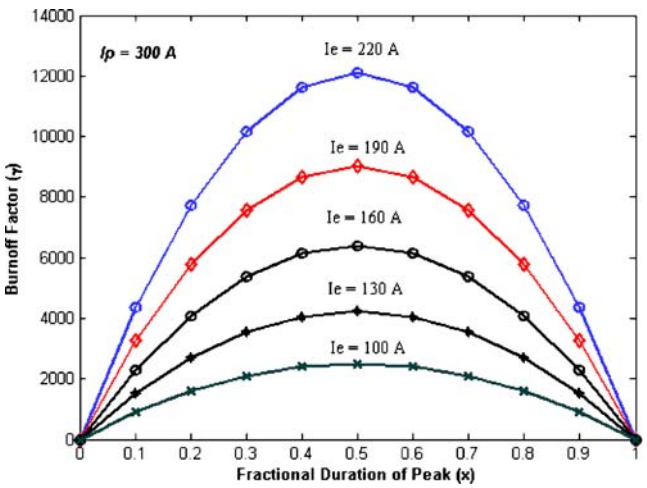

Fig. 5 Influence of fractional duration of peak (x=T_p.F) and excess current (I_e=I_p−I_b) on the burn-off factor (γ) for peak current of 300 A

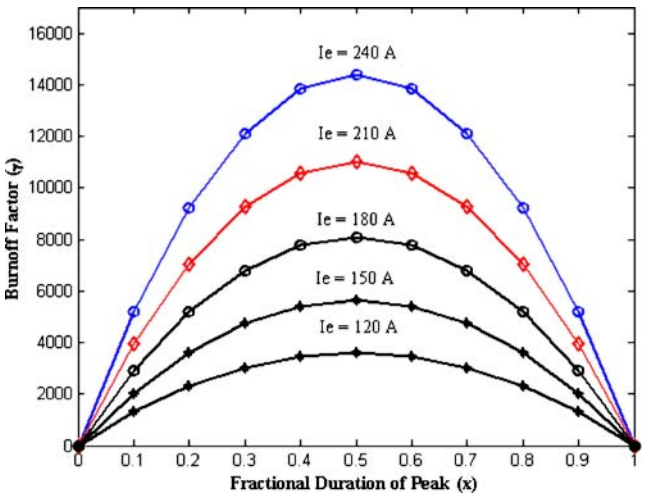

Fig. 6 Influence of fractional duration of peak (x=T_p.F) and excess current (I_e=I_p–I_b) on the burn-off factor (γ) for peak current of 320 A, keeping the other pulse condition values the same as for Fig. 5

and in determining the feed rate. However, at higher average currents it plays a significant role in determining the wire feed rate. The effect of base current on wire feed rate is presented in Fig. 12. It can be observed that, at the higher average currents, the influence of base parameter becomes more pronounced (i.e. the difference is more). Also, the difference in feed rates is more when the peak current value is lower compared to higher peak values and also the curve tends to be non-linear when the base parameter is taken into account whereas it is linear for the same set of conditions when the base current is neglected.

5.4 Prediction of gradient (S_m) between average current and wire feed rate

In fact, Eq. 12 shows that the wire feed rate is not directly proportional to the average current because the joule

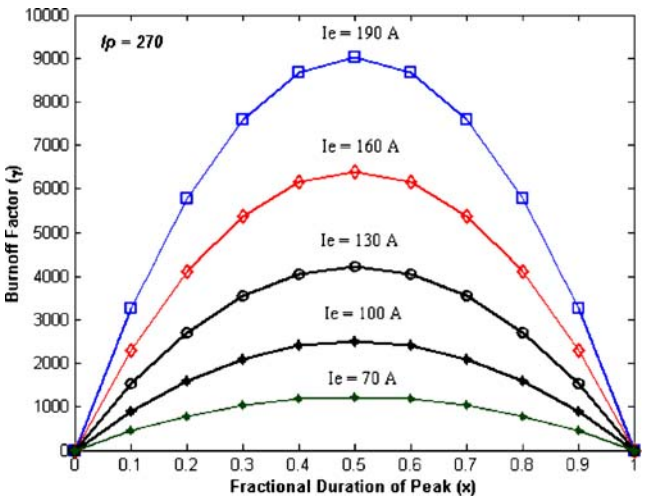

Fig. 7 Influence of fractional duration of peak (x=T_p.F) and excess current (I_e=I_p–I_b) on the burn-off factor (γ) for peak current of 270 A, keeping the other pulse condition values the same as for Fig. 5

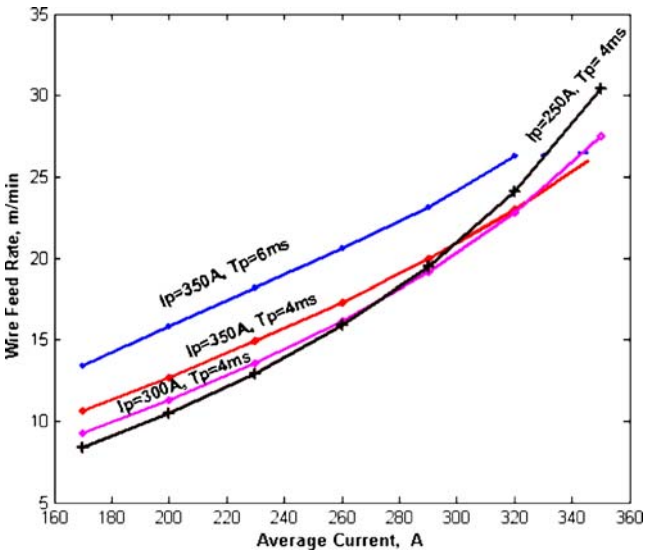

Fig. 8 Influence of peak parameters on wire feed rate

heating term becomes increasingly important at high average currents and for high resistivity wires [22]. However, Eq. 12 can be linearised if the joule heating term is considered to be proportional to average current. To do this a relationship between wire feed rate and the volume of wire melted is used such that:

$$\frac{V_d}{T} = WA \tag{18}$$

Hence,

$$T = \frac{V_d}{WA} \tag{19}$$

where T is the pulse period in seconds, A is the wire cross-sectional area and V_d is the volume wire delivered in time T.

Hence from Eq. 12,

$$W = \alpha I_{av} + \beta L\left(I_p^2 T_p + I_p^2 T_b\right) T^{-1} \tag{20}$$

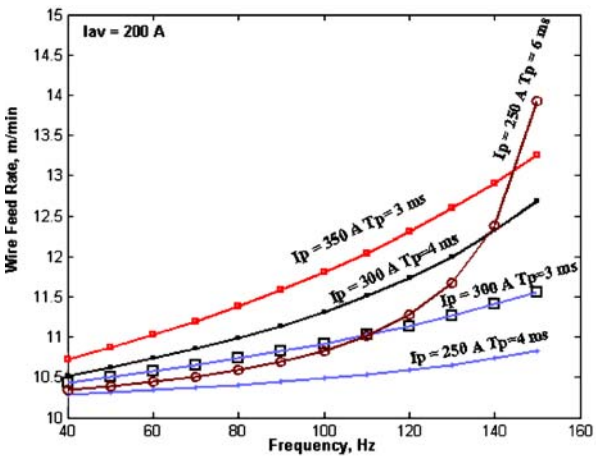

Fig. 9 Influence of frequency on wire feed rate for average current I_{av}=200 A

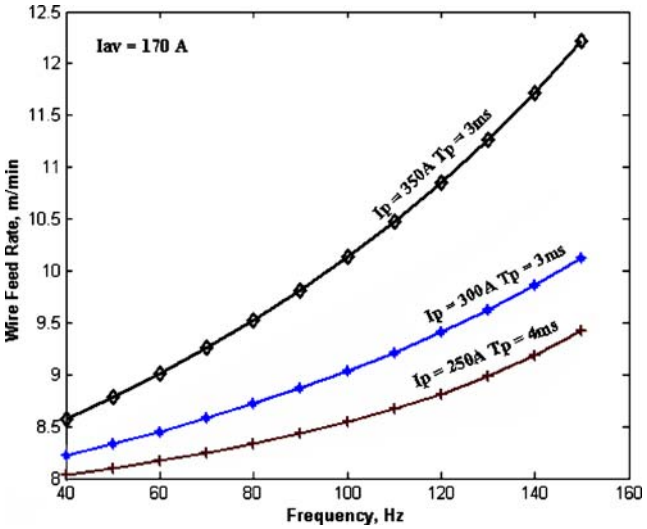

Fig. 10 Influence of frequency on wire feed rate for average current I_{av}=170 A

since $F=T^{-1}$

$$W = \alpha I_{av} + \beta L\left(I_p{}^2 T_p + I_p{}^2 T_b\right) W A V_d^{-1} \tag{21}$$

$$W = \frac{\alpha}{1 - \frac{\beta L A\left(I_p^2 T_p + I_b^2 T_b\right)}{V_d}} I_{av} \tag{22}$$

For simplification, neglecting base parameters,

$$W = \frac{\alpha}{1 - \frac{\beta L A I_p^2 T_p}{V_d}} I_{av} \tag{23}$$

i.e. $W=K.I_{av}$ where K is a constant given by

$$K = \frac{\alpha}{1 - \frac{\beta L A I_p^2 T_p}{V_d}}$$

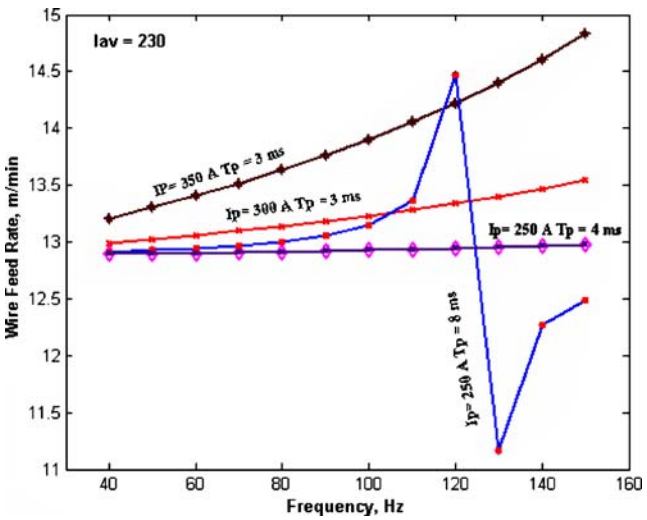

Fig. 11 Influence of frequency on wire feed rate for average current I_{av}=230 A

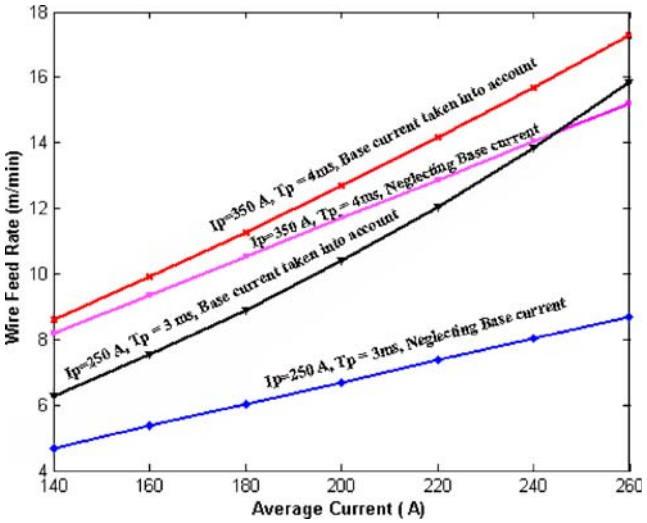

Fig. 12 Effect of base current on wire feed rate

For a constant wire diameter, the gradient S_m, as a function of peak current, peak time, volume of wire melted per pulse and stick-out, can be predicted from Eq. 24 [22]:

$$S_m = \frac{\alpha}{1 - \frac{\beta L\left(I_p^2 T_p + I_b^2 T_b\right)}{V_d}} \tag{24}$$

Figure 13 shows a linear relationship between average current and wire feed rate, as predicted by Eq. 23, for peak current of 300 A, peak pulse duration of 2.5 msec, droplet volume of 1.1 mm^3, and electrode extension of 20 mm. The value of gradient measured from Fig. 13 is 0.83 compared with the value of 1.02, the predicted average value of gradient using Eq. 24.

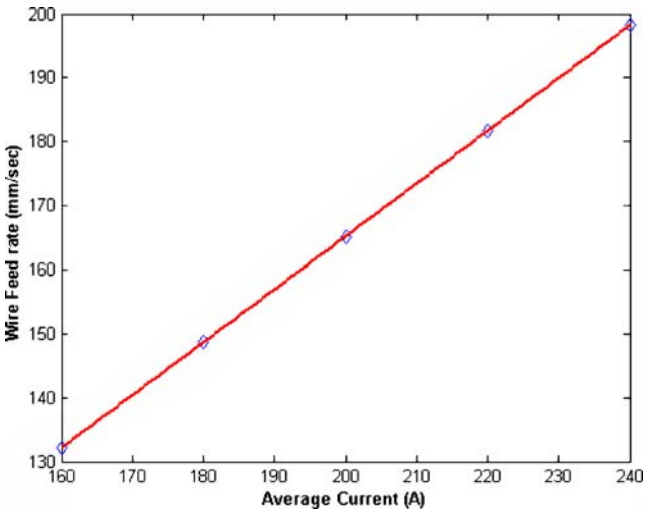

Fig. 13 Relationship between average current and wire feed rate and influence of current on wire feed rate predicted using Eq. 23: wire 1.2 mm dia, volume of wire melted=1.1 mm^3, I_p=300 A, T_p=2.5 ms

6 Conclusions

1. The values of arc resistance heating constant (α) and wire resistance heating constant (β) for 317L austenitic stainless steel wire are found to be 0.2998 mm /A/sec and 0.000138 A^{-2} sec^{-1}, respectively.
2. It was observed that the pulse parameters have significant influence on wire feed rate. Among the pulse parameters, the peak parameters have more influence on the wire feed rate; however, the effect of base parameters can not be neglected. Also, it was observed that the higher the excess current is, the higher the feed rate is.

Acknowledgements The authors wish to thank the All India Council for Technical Education, New Delhi and University Grant Commission, New Delhi, India for their financial support for procuring the equipment and materials. The authors also wish to thank Böhler Thyssen Welding, Austria, for sponsoring the 317L flux cored wire to carry out this investigation.

References

1. Boughton, Lucey JA (1965) The use of pulsed current to control metal transfer in welding. Br Weld J 4:159–166
2. Allum CJ (1983) MIG welding—time for a reassessment. Met Constr, June 347–353
3. Needham JC (1965) Pulse controlled consumable electrode welding arcs—general principles and operating characteristics. Br Weld J 4:191–197
4. Rajasekaran S (1999) Weld bead characteristics in pulsed GMA welding of Al-Mg alloys. Weld J 78(12):397–407
5. Amin M (1983) Pulse current parameters for arc stability and controlled metal transfer in arc welding. Met Constr, May 272–377
6. Stanzel K (2001) Pulsed GMAW cuts cycle time by 600 percent. Weld Design Fabr, April 85–87
7. Jilong M, Apps RL (1983) New MIG process results from metal transfer mode control. Weld Met Fabr, May 168–175
8. Raja A (1998) Flux core stelliting by pulsed MAG welding. WRI J 19(3):98–101
9. Elliott Sue (1985) Using synergic MIG successfully. Met Constr, March 148–151
10. Rajasekaran S (2000) Surface topography of pulsed current gas metal arc clads. Surf Eng 16(6):495–500
11. Vilarinho LO, Scotti A (2000) An alternate algorithm for synergic pulsed GMAW of aluminum. Aust Weld J 45:36–44
12. Weber Jeff (1982) Pulsed GMAW a plus for midwestern metal worker. Weld J 62(11):51–52
13. Essers WG, Van Gompal (1984) Arc control with pulsed GMA welding. Weld J 64(6):26–32
14. Bosworth MR (1991) Effective heat input in pulsed gas metal arc welding with solid wire electrodes. Weld J 70(5):111-s–117-s
15. Kim YS, Eagar TW (1993) Metal transfer in pulsed current gas metal arc welding. Weld J 72(7):279–287
16. Ghosh PK, Gupta PC (1996) Use of pulse current MIG welding improves the weld characteristics of Al-Zn-Mg Alloy. Indian Weld J, April 24–32
17. McGlone (1982) Weld bead geometry prediction—a review. Metal Constr, July 378–384
18. Pixley M, Kemppi (1989) Power sources for pulsed MIG welding. Joining and Materials, June 268–271
19. Norrish J (1987) What is synergic MIG? Weld Met Fabr 227–232, July
20. Rajasekaran S, Kulkarni SD et al (1998) Droplet detachment and plate fusion characteristics in pulsed current gas metal arc welding. Weld J 77(6):254–269
21. Subramaniam S, White DR, Jones JE, Lyons DW (1999) Experimental approach to selection of pulsing parameters in pulsed GMAW, AWS. Weld J 78(5):166–172
22. Smati Z (1986) Automatic pulsed MIG welding. Met Constr, Jan 38R–44R
23. French IE, Bosworth MR (1995) A comparison of pulsed and conventional welding with basic flux cored and metal cored welding wires. Weld J 74(6):197–205
24. Cornu J (1988) Advanced welding systems: consumable electrode processes. IFS, United Kingdom
25. Rajasekaran S (1997) Method of selecting the most suitable combination of parameters in pulsed current gas metal arc welding process. Proceedings of the international conference on advances in mechanical and industrial engineering, Roorkee, India, 6–8 Feb, pp 1115–1122
26. Collard JF (1998) Adaptive pulsed GMAW control: the digipulse system. Weld J 77(11):35–38
27. Murray PE (2002) Selecting parameters for GMAW using dimensional analysis. Weld J 81(7):125–131
28. Kim IS, Son KJ, Yang YS, Yaragada PKDV (2003) Sensitivity analysis for process parameters in GMA welding process using a factorial design method. Int J Mach Tools Manuf 43:763–769
29. Ramasamy S et al (2002) Design of experiments study to examine the effect of polarity on stud welding. Weld J 81 (2):19–26
30. Gosh PK, Gupta PC, Goyal VK (1998) Stainless steel cladding of structural steel plate using the pulsed current GMAW process. Weld J 77(7):307–314
31. Amin M, Naseer A (1987) Synergic control in MIG welding 2—power current controllers for steady DC open arc operation. Met Constr, June 331–340
32. Zhu et al (1997) Theoretical prediction of the start-up phase in GMA welding. Weld J 76(7):229–234
33. Amin M (1981) Synergic pulse MIG welding. Met Constr, June 349–353
34. Montgomery DC (1991) Design and analysis of experiments, 3rd edn. Wiley, New York
35. Ferraresi VA, Figueiredo KM, Hiap O (2003) Metal transfer in the aluminum gas metal arc welding. J Braz Soc Mech Sci Eng XXV (3):229–234
36. Palani PK, Murugan N (2006) Selection of parameters of pulsed current gas metal arc welding. J Mater Process Technol 172:1–10
37. Palani PK, Murugan N (2006) Metal transfer and burn off characteristics of pulsed current gas metal arc welding: a review. Int J Joining Mater (in press)
38. Lambert JA (1989) Assessment of the pulsed GMA technique for tube attachment welding. Weld J 68(2):35–43
39. Amin M, Naseer A (1987) Synergic control in MIG welding 1—parametric relationships for steady DC open arc operation. Met Constr, January 331–340
40. Allum CJ, Quintino L (1985) Control of fusion characteristics in pulsed current MIG welding. Met Constr, April 242R–245R
41. Needham JC, Carter AW (1965) Material transfer characteristics with pulsed current. Br Weld J 5:229–241
42. Subramaniam et al (1998) Droplet transfer in pulsed gas metal arc welding of aluminum. Weld J 77(11):458–463